Published in final edited form as:
J Control Release. 2016 May 10; 229: 120–129. doi:10.1016/j.jconrel.2016.03.029.

Targeted Delivery of siRNA to Activated T Cells via Transferrin-Polyethylenimine (Tf-PEI) as a Potential Therapy of Asthma

Yuran Xie[1], **Na Hyung Kim**[1], **Venkatareddy Nadithe**[1], **Dana Schalk**[1,2], **Archana Thakur**[1,2], **Ayşe Kılıç**[3], **Lawrence G. Lum**[1,2], **David JP Bassett**[1], and **Olivia M Merkel**[1,2,4]

[1]Wayne State University, Detroit, MI, United States of America

[2]Karmanos Cancer Institute, Detroit, MI, United States of America

[3]Philipps-Universität Marburg, Marburg, Germany

[4]Ludwig-Maximilians Universität München, Munich, Germany

Abstract

Asthma is a worldwide health problem. Activated T cells (ATCs) in the lung, particularly T helper 2 cells (Th_2), are strongly associated with inducing airway inflammatory responses and chemoattraction of inflammatory cells in asthma. Small interfering RNA (siRNA) as a promising anti-sense molecule can specifically silence inflammation related genes in ATCs, however, lack of safe and efficient siRNA delivery systems limits the application of siRNA as a therapeutic molecule in asthma. Here, we designed a novel pulmonary delivery system of siRNA, transferrin-polyethylenimine (Tf-PEI), to selectively deliver siRNA to ATCs in the lung. Tf-PEI polyplexes demonstrated optimal physicochemical properties such as size, distribution, zeta-potential, and siRNA condensation efficiency. Moreover, *in vitro* studies showed significantly enhanced cellular uptake and gene knockdown mediated by Tf-PEI polyplexes in human primary ATCs. Biodistribution of polyplexes in a murine asthmatic model confirmed that Tf-PEI polyplexes can efficiently and selectively deliver siRNA to ATCs. In conclusion, the present work proves the feasibility to target ATCs in asthma via Tf receptor. This strategy could potentially be used to design an efficient siRNA delivery system for asthma therapy.

Keywords

siRNA delivery; pulmonary delivery; asthma; transferrin; polyethylenimine (PEI)

1 Introduction

Asthma is a chronic inflammatory disease in the respiratory tract affecting 300 million people globally (2014, Global Asthma Report) [1]. Current therapies of asthma make use of a combination of inhaled corticosteroids and quick relief medications, which can efficiently control asthmatic symptoms in the majority of patients. However, there are 5-10% asthmatic patients whose disease remains poorly controlled and whose lives are threatened. Therefore,

Corresponding author: Prof. Dr. Olivia Merkel, Department of Pharmacy, LMU München, Butenandtstr. 5-13 (Haus B), D 81377 München, Germany, Tel. 089 2180 77025, FAX 089 2180 77020 Olivia.merkel@LMU.de.

Europe PMC Funders Author Manuscripts

an alternative therapy for asthma is needed. Inflammation in asthma is driven by an infiltration of inflammatory cells such as activated T cells (ATCs), eosinophils and mast cells. Among infiltrated inflammatory cells, ATCs, specifically, T helper 2 cells (Th_2) play a critical role in orchestrating pathological processes of asthma via the production of Th_2 cytokines [2–4]. Therefore, blockage of the functions of Th_2 interleukins (e.g. IL-5 [5]) or silencing of upstream transcription factors which promote the production of Th_2 interleukins (e.g. GATA-3 [6]) have been investigated as potential therapies of difficult-to-treat asthma.

RNA interference (RNAi) is a process of sequence specific degradation of messenger RNA (mRNA). Small interfering RNA (siRNA) is involved in RNAi and can efficiently, specifically and post-transcriptionally silence genes. Therefore, synthetic siRNA is anticipated to be a solution to various diseases [7, 8]. Substantial investigations have been undertaken for applying siRNA to silence asthma related genes in Th_2 cells (e.g. IL-5 [9] and GATA-3 [10]). Nevertheless, safe and effective delivery of siRNA is facing several challenges. The hurdles are to overcome various physiological barriers including emzymatic degradation, non-specific binding to non-target tissues or cells, negatively charged cellular membranes, endosomal escape after endocytosis, and many more [11]. Moreover, delivery of siRNA to Th_2 cells is particularly difficult because T cells are in general resistant to non-viral vector-based transfection methods [12]. T cells do not actively endocytose nanoparticles because they do not express caveolin and are devoid of caveolae [13, 14]. Conventional transfection approaches of T cells are viral delivery systems [15] or electroporation [16]. However, the fabrication of viral vectors is time and cost consuming, and their potential safety issues limit their clinical application [17]. On the other hand, electroporation is not a suitable method for *in vivo* administration of siRNA [18]. Various delivery systems have been discovered to target T cells, including CD3 targeted polyethylenimine (PEI) [19], CD40L targeted liposomes [20], CD7 targeted chitosan [21] or oligo-arginine [22]. However, their efficiency and potential systemic side effects for asthma therapy remain to be tested. Since CD7 and CD3 are pan T cell surface antigens and since nanomedicines targeting these receptors were all applied through systemic administration in their respective *in vivo* studies, it would be expected to observe side effects with these strategies.

In order to avoid potential systemic side effects and to increase the selectivity for activated T cells, the key mediators in asthma pathogenesis and development, our group has developed a pulmonary siRNA delivery system based on transferrin-polyethylenimine (Tf-PEI). This ligand-polymer conjugate takes advantage of the increased expression of transferrin receptors (TfR) on T cells after activation [23]. TfR is a membrane protein expressed at low level on most cells and can bind to the iron transport glyco-protein Tf, which consequently triggers fast internalization [24]. Previously, we showed that only activated primary T cells take up siRNA delivered by Tf-PEI, while naïve T cells with a basal level of TfR expression cannot be reached efficiently with the Tf-PEI conjugate for siRNA delivery [25]. Low molecular weight PEI (5k Da) is used as a carrier of siRNA to facilitate cellular internalization and endosomal escape [26] with minimal toxicity [27, 28]. N-succinimidyl 3-(2-pyridyldithio) propionate (SPDP) as a crosslinker can introduce a disulfide bond between Tf and PEI. Disulfide bonds are stable extracellularly but can be reduced in the endosome

compartment [29] and allow PEI/siRNA polyplexes to be released from the Tf/TfR complex prior to rapid recycling of TfR.

The aim of this study was to develop a pulmonary delivery system that can selectively and efficiently deliver siRNA to activated T cells in the lung and could be potential applied for asthma therapy. In the present work, Tf-PEI exhibited optimal physicochemical properties in terms of siRNA condensation efficiency, size, zeta-potential and stability in the presence of lung surfactant and mucin. *In vitro* studies revealed that Tf-PEI can efficiently deliver siRNA to primary human ATCs or Jurkat cells and mediated significant gene knock down. Biodistribution of Tf-PEI polyplexes formulated with fluorescently labeled siRNA in a murine asthmatic model after intratracheal administration confirmed that Tf-PEI can selectively deliver siRNA to ATCs *in vivo*.

2 Material and Method

2.1 Materials

N- succinimidyl 3-(2-pyridyldithio) propionate (SPDP) was purchased from Pierce (Rockford, IL), SYBR Gold dye and Lipofectamine 2000 were obtained from Life Technologies (Grand island, NY), branched low molecular weight (LMW) 5k Da PEI (Lupasol® G100) was from BASF (Ludwigshafen, Germany), murine transferrin, picrylsulfonic acid solution (TNBS, 5% w/v), Dulbecco's phosphate buffered saline (PBS), dimethyl sulfoxide (DMSO), ethylenediaminetetraacetic acid disodium salt dehydrate (EDTA), type II mucin from porcine stomach, and albumin from chicken egg white (OVA) were bought from Sigma-Aldrich (St. Louis, MO). Chloroquine diphosphate was from MP biomedicals (Santa Ana, California), human holo-transferrin was purchased from EMD Millipore (Billerica, MA), 1,4-Dithio-DL-threitol (DTT, 99%) was obtained from Alfa Aesar (Ward Hill, MA). Amine modified siRNA (5´- pACCCUGAAGUUCAUCUGCACCACcg, 3´-ACUGGGACUUCAAGUAGACGUGGUGGC), human glyceraldehyde- 3- phosphate-dehydrogenase (GAPDH) siRNA (5´-pGGUCGGAGUCAACGGAUUUGGUCgt, 3´-UUCCAGCCUCAGUUGCCUAAA- CCAGCA), and scrambled siRNA (5´-pCGUUAAUCGCGUAUAAUACGCGUat, 3´-CAGCAAUUAGCGCAUAUUAUGCGCAUAp) were purchased from Integrated DNA Technologies (Coralville, IA) (indication of modified nucleotides: "p" denotes a phosphate residue, lower case bold letters are 2´-deoxyribonucleotides, capital letters are ribonucleotides, and underlined capital letters are 2´-*O*-methylribonucleotides). A 0.4% trypan blue solution in phosphate buffered saline was purchased from HyClone GE healthcare (Buckinghamshire, UK).

2.2 Synthesis of transferrin-polyethylenimine (Tf-PEI) conjugate

For the first reaction, 5k PEI (1 mg/ml) dissolved in HEPES buffered saline (HBS) (20 mM HEPES, 150 mM NaCl, pH=7.5) was mixed with a 10-fold molar excess SPDP (20 mM) in dry DMSO and stirred for overnight. A Tf solution (10 mg/ml, human or murine) was dissolved in HBS and stirred with a 5-fold molar excess SPDP for 2 h. Purification of PEI-SPDP and Tf-SPDP were performed via 3,000 or 10,000 MWCO centrifugal filters (Millipore, Billerica, MA) with HBS/1 mM EDTA (pH=7.1), respectively. To estimate the

concentration of SPDP in the PEI-SPDP solution, 100 μl of 50-fold diluted PEI-SPDP solution was reacted with 1 μl of a 150 mM DTT solution for 30 min, and the pyridon-2-thion release was measured spectrophotometrically at 343 nm in a 96-well UV plate (Corning). Subsequently, a 10-fold molar excess DTT was mixed and reacted with the remaining PEI-SPDP under nitrogen protection for 2 h. Reduced PEI-SPDP was purified by 3,000 MWCO centrifugal filters with HBS/20 mM EDTA (pH=7.1). For the coupling reaction, Tf-SPDP was added stepwise to PEI-SPDP and stirred overnight at 4 C°. Purification of Tf-PEI was achieved on an ÄKTA FPLC system (GE healthcare) equipped with 2 connected 1 ml HiTrap SP HP cation exchange column (GE healthcare) as described before [30]. Free Tf was washed out with 0.5 M NaCl/20mM HEPES and Tf-PEI was eluted after initial binding to the column after switching to 3 M NaCl/20 mM HEPES. Further purification and desalination was performed by 30,000 MWCO centrifugal filters (Millipore) with HBS. The concentration of Tf in the Tf-PEI conjugate was determined spectrophotometrically at 280 nm. To determine the concentration of PEI in Tf-PEI, a standard curve was generated by diluting PEI in a solution containing a constant concentration of Tf. According to the standard curve, the concentration of PEI in Tf-PEI conjugate was assessed at wavelength 405 nm using a TNBS assay [31].

2.3 Preparation of polyplexes

Polyplexes were prepared in either HBS or 5% glucose. An equal volume of Tf-PEI or PEI was added to a defined amount of siRNA solution to yield different amine to phosphate ratios (N/P ratios) and incubated for 20 min before further measurement or transfection. Lipofecatmine 2000 (LF) lipoplexes preparation was performed according to the manufacturer's protocol. Briefly, every 10 pmol siRNA were formulated with 0.5 μl LF. The amount of PEI or Tf-PEI needed at different N/P ratio for 50 pmol siRNA were calculated according to the following equation: m (PEI in pg) = 50 pmol × 43.1 g/mol × N/P × 52 (protonable unit of PEI = 43.1 g/mol, number of nucleotides of 25/27mer siRNA = 52).

2.4 Hydrodynamic size and zeta-potential measurement

For the measurement of size, PEI or Tf-PEI polyplexes were prepared with 50 pmol siRNA in HBS at different N/P ratios. The total volume of 100 μl polyplexes was added into a disposal micro cuvette (Brand GMBH, Wertheim, Germany) and the size was measured using a Zetasizer Nano ZS (Malvern Instruments Inc., Westborough, MA). The measurement was set up at 173° backscatter angle and 15 runs were performed three times for each sample. For data analysis, 0.88 mPa*s for viscosity and 1.33 for refractive index were used with the Zetasizer Software (Malvern). Subsequently, polyplexes were diluted with Nanopure water (Thermo scientific) to 1 ml and transferred to a folded capillary cell (Malvern) and zeta-potential measurements were performed three times for each sample using the Zetasizer Nano ZS (Malvern).

2.5 SYBR gold dye binding assay

To measure siRNA condensation efficiency of the conjugates in comparison to the unmodified polymer, siRNA in 5% glucose was distributed in a FluoroNunc 96-wells white plate (Thermo Fisher Scientific, Waltham, MA) at a concentration of 50 pmol/50 μl per well followed by adding 50 μl of different concentration of either PEI or Tf-PEI to form

polyplexes at different N/P ratios. After 20 min incubation, 30 μl of 4 × SYBR gold solution was added to each well and incubated for 10 min in the dark. SYBR gold fluoresces when it intercalates with free siRNA but not if siRNA is not accessible due to condensation and protection by polymers. The fluorescence was quantified using a Synergy 2 multi-mode microplate reader (BioTek Instrument, Winooski, VT) at excitation wavelength of 485/20 nm and emission wavelength of 520/20 nm. Fluorescence of free siRNA (N/P=0) represents 100% of free siRNA.

To evaluate the stability of polyplexes, release of siRNA from polyplexes in presence of lung surfactant Alveofact® (Boehringer-Ingelheim, Germany) or mucin was determined by a modified SYBR gold assay [32]. While the surfactant assay measures siRNA release from polyplexes by surface-active phospholipids, the mucus assay determines polyplexes instability in presence of mucus glycoproteins. Tf-PEI and PEI polyplexes were prepared with siRNA at N/P 7.5 and distributed in a 96-well white plate at a concentration of 50 pmol siRNA/100 μl per well. After 15 min incubation, 50 μl of 4 × SYBR gold solution was added to each well and incubated for 10 min in the dark. Subsequently, 50 μl of a serial dilution of Alveofact® or mucin was added (final concentrations: 0, 0.0005, 0.005, 0.05, 0.25, 0.5 mg/ml) and incubated for additional 20 min in the dark before measurement of the fluorescence. To account for the autofluorescence of mucin, free siRNA samples were prepared in the presence of corresponding concentrations of mucin. The experiment was performed in replicates of three and fluorescence of free siRNA represents 100% siRNA release.

2.6 Cell culture

Peripheral blood mononuclear cells (PBMCs) were obtained from healthy donors (KCI protocol 2007-012). This protocol was approved by the Wayne State University Human Investigation Committee. PBMCs were cultured at a concentration of 10^6 cells/ml in RPMI-1640 with HEPES & L-Glutamine cell culture medium (Lonza, Walkersville, MD) supplemented with 10 % heat inactivated fetal bovine serum (v/v) (Sigma), 1 × penicillin/streptomycin (Corning, Corning, NY) and 2 mM L-Glutamine (Gibco® Thermo Fisher Scientific). Peripheral resting T cells in PBMCs were stimulated with anti-CD3 monoclonal antibody (OKT3, Ortho Biotech, Horsham, PA) at a final concentration of 20 ng/ml and expanded with 100 IU/ml human recombinant interleukin-2 (IL-2), Novartis). Jurkat cells, a human T lymphocytes cell line, were a kind gift from Dr. Larry H. Matherly (Karmanos Cancer Institute). Jurkat cells were cultured in the same media as primary T cells. All cells were grown at a humidified atmosphere with 5% CO_2 at 37 C°. Primary ATCs were frozen at −130 C° in 50% FBS, 40% growth media and 10% DMSO on different post-activation days for later experiment.

2.7 Immunofluorescent staining

Human ATCs, harvested on different post-activation days, or Jurkat cells were washed with PBS and 400,000 cells per sample were resuspended with 10 μl 50-fold diluted human FcR binding inhibitor (ebioscience, San Diego, CA) for 5 min on ice, followed by staining with 2 μl of PE labeled human CD71 antibody (OKT9, ebioscience) or PE labeled mouse IgG1 isotype control antibody (P3.6.2.8.1, ebioscience) for 30 min at 4 °C protected from light.

Afterward, cells were washed twice and resuspended with 400 μl ice cold PBS/2 mM EDTA before they were analyzed with an Attune® Cytometer (Life Technologies). The cellular suspensions were measured with 488 nm excitation and the emission filter set of 574/26 nm. On day 6 post-activation, ATCs were counterstained with a CD71 antibody and a PE-Cy7 labeled human CD3 antibody (UCHT1, Molecular probes). The samples were measured with 488 nm excitation and emission filter of 574/26 nm and 640 LP in an Attune® Cytometer (Life Technologies). A viable lymphocyte population was gated according to morphology based on forward and sideward light scattering within which 10,000 events were evaluated. All results are given as median fluorescent intensity (MFI). Data analysis was performed using Attune® cytometer software (Life Technologies).

2.8 Quantification of cellular uptake

Amine modified siRNA was labeled with succinimidyl ester (NHS) modified Alexa Fluor 488 (AF488) (Life technologies) following the manufacturer's protocol and purified by ethanol precipitation and spin column binding as described previously [33]. For uptake experiments, 50 pmol siRNA-AF488 was prepared with Tf-PEI or PEI in 5% glucose at different N/P ratios (N/P ratio: 5, 7.5, 10, 15, 20) or with LF. The day before the experiment, 400,000 ATCs or Jurkat cells were seeded in 96 well plates (Thermo scientific) at a concentration of 2×10^6cells/ml and transfected with the polyplexes/lipoplexes for 24 h. Samples were washed three times and resuspended in 400 μl PBS/2 mM EDTA. For initial experiments, ATCs were transfected with low N/P ratio treatment groups were analyzed using a BD LSR II flow cytometer (BD bioscience, San Jose, CA). For later experiments, ATCs or Jurkat cells were transfected with high N/P ratios (10, 15, 20, or 5, 10, 20), and samples were analyzed using an Attune® Cytometer (Life Technology) with 488 nm excitation and emission filter of 530/30. The cells were gated according to morphology within which 10,000 events were evaluated. For trypan blue quenching assays, ATCs were treated by Tf-PEI or PEI polyplexes at N/P 20 or LF lipoplexes for 24 h. Each sample was divided into two halves; one half was washed once with 0.4% trypan blue to quench the extracellular fluorescent signal then washed with cold PBS/2 mM EDTA three times, the other half was only washed three times. Samples were resuspended in 400 μl PBS/2 mM EDTA and analyzed with an Attune® Cytometer (Life Technology) as described above.

2.9 *In vitro* GAPDH gene knockdown

For gene silencing experiments, 400,000 ATCs or Jurkat cells were seeded in a 96 well plate and triplicates of samples were treated with Tf-PEI, PEI or LF polyplexes/lipoplexes prepared with 50 pmol for ATCs or 100 pmol for Jurkat cells for 24 h using either hGAPDH siRNA or scrambled siRNA at N/P 15. Cells were harvested and processed to isolate total RNA using the PureLink™ RNA mini kit (Life techonologies) according the manufacturer's protocol with DNase I digestion (Thermo scientific). Synthesis of cDNA from total RNA and PCR amplification were performed with Brilliant III ultra-fast SYBR® green QRT-PCR master mix kit (Agilent Technologies, Santa Clara, CA) using a Stratagene Mx 3005P (Agilent Technologies). Cycle threshold (Ct) values were determined by MxPro software (Agilent Technologies). A standard curve including 5 points was made from a 1:5 serial dilution of an untreated sample and assigned concentrations of each point (1, 0.2, 0.004, 0.0008, 0.00016) were plotted vs. their corresponding Ct values. The gene expression of

GAPDH was normalized by the expression of β-actin. Hs_GAPDH_2_SG primers for GAPDH and Hs_ACTB_2-SG primers for β-actin (Qiagen, Valencia, CA) were used in experiment.

2.10 Cellular distribution of polyplexes in a murine asthma model

All animal experiments were approved by a Wayne State University Institutional Animal Care and Use Committee. Balb/c mice were purchased from Charles River Laboratories (Boston, MA) and used at 5 weeks' age. The murine asthma model was established as described before [34]. Briefly, animals were sensitized by intraperitoneal (i.p.) injection of 0.2 ml suspension of ovalbumin (OVA) and $Al(OH)_3$ (10 μg OVA and 2 mg $Al(OH)_3$) on day 0 and day 14 (Figure 8 A). On days 24, 25, and 26, mice were challenged by inhalation of aerosolized 1% OVA for 1 h to establish experimental asthma while mice that inhaled saline were used as healthy control group. On days 35, 36, 37 and 38, mice were intratracheally (i.t) instilled (under ketamine/xylazine anesthesia) with 50 μl Tf-PEI or PEI polyplexes, prepared with 750 pmol Alexa Fluor 647 (Life technologies) labeled siRNA at N/P 7.5, or free siRNA-AF647 as control. On days 36, 37 and 38, before the i.t. administration, a second series of daily OVA or saline challenges was performed. On day 39, noninvasive lung function of animals was determined by whole-body plethysmography. Changes in the delayed pause in breathing as an indicator of altered bronchial responsiveness to increasing aerosol challenge concentrations of β-methacholine was monitored (Buxco Electronics Inc., Wilmington, DE) [35]. On day 40, all animals were sacrificed under i.p. ketamine/xylazine anesthesia, exsanguinated and perfused with PBS. bronchoalveolar lavage fluid (BALF) and BALF cells were collected [36] and lung cell suspensions were prepared as reported before [37]. BALF cells and lung suspension cells were counterstained with PerCP-Cy 5.5 labeled anti-CD45 (30-F11, ebioscience), PE-Cy7 labeled anti-CD4 (GK1.5, eBioscience), a primary anti-prosurfactant protein C antibody (proSPC) (1:100, abcam), pacific blue labeled goat anti-mouse IgG secondary antibody (1:100, Life Technologies), pacific orange labeled anti-F4/80 (invitrogen), APC-Cy7 labeled anti-CD19 (MB19-1, molecular probes), and PE labeled anti-CD49d (R1-2, Molecular Probes) antibodies following the manufacturer's protocols. Cell differentiation was performed on a BD LSR II flow cytometer (BD bioscience). The staining and gating strategy can be found in the supplementary materials. The different cell populations of macrophage/monocytes (F4/80+), T cells (CD4+, F4/80−), eosinophils (CD4−, CD49d+), and epithelial Type II pneumocytes (proSPC+) were gated, and the MFI of siRNA-AF647 in all different cell populations was quantified. To quantify cellular uptake of polyplexes in T cells only, lung suspension cells were stained with a PE-Cy7 labeled anti-CD4 antibody. T cells were gated based on morphology, and the MFI of siRNA-AF647 was quantified within CD4+ cells by an Attune® Cytometer (Life Technology). The concentration of interleukin-5 (IL-5) and interleukin-13 (IL-13) in BALF was determined by the mouse cytokine 20-plex panel (Invitrogen) using a Bio-Plex® System (Bio-Rad Lab., Hercules, CA) following the manufacturer's protocol. Interleukin concnetrations below the detection limitation were reported as 0 pg/ml.

Europe PMC Funders Author Manuscripts

Europe PMC Funders Author Manuscripts

2.11 Statistics

All results are given as mean value ± standard deviation (SD). One-way ANOVA with Bonferroni posthoc post-test, two-way ANOVA and calculation of area under the curve (AUC) were performed in GraphPad Prism software (Graph Pad Software, La Jolla, CA).

3 Result and Discussion

3.1 Synthesis Outcome

Transfection efficiency and toxicity of PEI are often correlated to its molecular weight [38]. Here, low molecular weight PEI (5k Da) was chosen to decrease potential toxicity and non-specific transfection efficacy. Holo-Tf preferentially binds to TfR [24] and has been reported as a targeting ligand for various diseases involving TfR overexpression using lipid-based [39] or polymer-based delivery systems carrying pDNA [40, 41], siRNA [42] or oligonucleotides [43] for anti-sense therapy. To target ATCs, holo-Tf was conjugated to PEI to increase the intracellular internalization efficiency. As shown in Figure 1, holo-Tf and 5k PEI were reacted with the bifunctional crosslinker SPDP, respectively, and PEI-SPDP was activated by the reducing reagent DTT. Activated PEI-SPDP* (see Figure 1) was conjugated to Tf-SPDP to yield Tf-PEI. The final concentration of Tf was determined by UV absorbance at 280 nm, and the concentration of PEI was assessed by TNBS assay. The resulting molar ratio of Tf to PEI was approximately 1.5 : 1. Due to the difference of molecular weights between Tf (80 kDa) and LMW PEI (5 kDa), higher coupling degrees were not expected and could in fact be disadvantageous for the interaction between PEI amines and siRNA phosphate groups.

3.2 siRNA condensation of Tf-PEI

The siRNA condensation efficiency of a polymer is an important property to evaluate the suitability of a carrier for siRNA. To determine whether the presence of Tf would affect the ability of PEI to condense siRNA, the condensation efficiency of Tf-PEI was determined by SYBR® Gold assays, and unmodified 5k PEI was used as a control. SYBR gold is a nucleic acid-intercalating fluorescent dye. When siRNA is condensed by polymer and becomes inaccessible to SYBR gold, consequently a decrease of fluorescence is observed. As shown in Figure 2, PEI can completely condense and protect the siRNA at N/P 5 which was consistent with previous reports [44]. On the other hand, both human and mouse Tf-PEI condensed siRNA to 80% at N/P 5, and complete condensation of siRNA was observed at N/P 7.5. The difference may be due to steric hindrance of Tf which impacts the interaction between siRNA and the primary amines in PEI. It also needs to be taken into consideration that by coupling Tf to PEI, a few primary amines would be expected to no longer be available for interaction with siRNA. However, the influence of the Tf modification on condensation efficacy of the conjugate is limited, with full condensation still achievable at a comparably low N/P ratio of 7.5.

3.3 Hydrodynamic diameter and zeta potential

Optimal physicochemical properties of polyplexes such as size and surface charge can facilitate efficient siRNA delivery *in vitro* and *in vivo*. Therefore, Tf-PEI or PEI polyplexes,

prepared with the same amount siRNA in HBS buffer at different N/P ratios, were fully characterized for size, polydispersity index (PDI) and zeta potential by dynamic light scattering and laser Doppler anemometry. As shown in Figure 3A, Tf-PEI formulations demonstrated small sizes ranging from 72 to 197 nm and PDIs ranging from 0.24 to 0.39. In comparison, PEI formed larger particles of 1133 nm to 1595 nm in size with PDI of approximately 0.3. Both formulations demonstrated acceptable size distributions with PDIs mostly below 0.3 indicating homogeneous morphology and little aggregation which is an important factor for successful transfection. Size of polyplexes is another key factor for efficient transfection, and small sizes (<200 nm) of the Tf-PEI polyplexes could ensure higher stability and better intracellular uptake efficiency especially into ATCs compared with large PEI polyplexes (>1000 nm) [45]. Considering that Tf is a very soluble glycoprotein, it is possible that Tf decorates the surface of Tf-PEI polyplexes and a resulting steric stabilization of Tf contributes to the much smaller size of the particles [40]. Consistent with this hypothesis, it has been reported that low molecular weight PEI tends to form large particles with siRNA [46] and a tendency of aggregation of PEI has been observed when preparing polyplexes in high ionic strength buffers such as HEPES buffered saline [40].

Zeta potentials of both Tf-PEI and PEI polyplexes increased with increasing N/P ratio (Figure 3B). Tf-PEI polyplexes displayed negative charges in the range of −20 to −7 mV which is in agreement with the assumption that the negatively charged Tf may shield the positive charges of PEI and is located on the surface of the polyplexes, resulting in an overall negative zeta potential [47]. On the other hand, except at N/P 2 where the zeta potential was −28.6 ± 3.9 mV, all PEI formulations showed slightly positive charges in the range from 8.5 mV to 26 mV. Due to the relatively “rigid” structure of short duplex siRNA and the fact that not all positively charged groups in PEI are sterically available to interact with siRNA, most of the siRNA may be on the surface of the polyplexes at a low excess of polymer, i.e. N/P 2. This could explain why a negative charge was observed at N/P 2. At higher N/P ratios, excess amount of PEI more efficiently interacts with the negative charges of siRNA resulting in positive zeta potentials of the polyplexes. Positive zeta potentials of polyplexes may hamper their penetration through lung mucus and surfactant which have negative charge [48] and also increase their chance of non-specific delivery via adsorptive endocytosis. Additionally, multiple pulmonary administrations of positively charged nanoparticles can increase local and systemic toxicity, while in comparison, anionic nanoparticles are well tolerated [49]. Therefore, we hypothesize that Tf-PEI polyplexes would be a more efficient and safe pulmonary administrated system than PEI.

3.4 Stability of polyplexes in the presence of lung surfactant

The instability of polyplexes in the blood stream limit their suitability for systemic administration. To overcome this challenge, pulmonary delivery is favorable for the treatment of lung diseases due to the large application area, the absence of serum proteins, and the reduced nuclease activity [50]. However, there are other biological barriers associated with using the airway route that need to be overcome to deliver siRNA to the lung. If epithelial cells in the upper airway are to be targeted, polyplexes need to penetrate a mucus layer before they reach the epithelium. In asthma therapy, polyplexes are mostly expected to be delivered to the deep lung, where the alveolar surface is covered by lung

surfactant which presents another barrier [48]. To investigate the stability of polyplexes in the lung, a modified SYBR® Gold assay was performed in the presence of lung surfactant Alveofact® or mucin and released siRNA was quantified. Tf-PEI polyplexes demonstrated higher stability compared with PEI polyplexes at increasing concentrations of mucin (0.0005 - 0.5 mg/ml) (Figure 4A). Similarly, at low concentrations of surfactant (0.0005 - 0.05 mg/ml), the ability of Tf-PEI to retain siRNA was also better than that of PEI. Only 1% siRNA release from Tf-PEI polyplexes but 4.3% from PEI polyplexes was observed at 0.05 mg/ml. At a concentration of 0.25 mg/ml, PEI and Tf-PEI polyplexes released 10.9% and 10.2% siRNA, respectively. As described above, there are indications that Tf is located on the surface of the polyplexes and consequently shields PEI/siRNA from interaction with surfactant or mucin. In contrast, at the highest concentration of surfactant (0.5 mg/ml), PEI more efficiently retained siRNA than Tf-PEI (Figure 4B). While 13.5% of siRNA were released from PEI, 16.2% of siRNA were released from Tf-PEI polyplexes. High concentration of surfactant may induce structural changes in Tf, as a result, the ability to retain siRNA in the polyplex simply depends on electrostatic interaction between siRNA and PEI. It is expected that Tf-PEI polyplexes would release more siRNA since unmodified PEI demonstrated slightly better ability to condense siRNA compared with Tf-PEI. In 2009, we reported also that PEGylated PEIs release siRNA more efficiently than unmodified PEI [32]. It should be noted that in 2009, 25 kDa PEI was described, whereas here we used 5 kDa PEI which showed slightly lower stability in presence of surfactant and mucin compared to 25 kDa PEI complexes. However, the studied concentrations of surfactant, of which predominant composition is phospholipids (up to 70% being dipalmitoyl phosphatidylcholine (DPPC)) [51], are much higher than that in a reported simulated lung fluid (0.02% (w/v) DPPC), used for dissociation tests of inhaled pharmaceutical formulations [52]. At physiological surfactant concentrations, Tf-PEI polyplexes therefore seem to exhibit enhanced stability compared to PEI polyplexes. This observation could lead to beneficial stability after aerosol deposition in the peripheral airways. On the other hand, 91% and 97% of siRNA, respectively, were released from Tf-PEI and PEI polyplexes at a very high concentration of 0.5 mg/ml mucin. In comparison, complexes of PEGylated 25 kDa PEI which mediated highly efficient gene knockdown in the lung showed about 30% siRNA release at mucin concentrations as low as 0.33 mg/ml [32]. Instability of siRNA polyplexes at exaggerated mucin concentrations therefore seem not to hamper efficient gene knockdon at physiological conditions. While surfactant is only present in the alveolar region, mucus lines in the upper and bronchial airways where the polyplexes are expected to mediate their therapeutic effects. Based on our experiments, mucus stability of future nanocarriers should be optimized. However, it is possible that stability in presence of surfactant plays a more important role in vivo where Tf-modification of the polyplexes was advantageous. Therefore, we hypothesize that Tf could protect the polyplexes for sufficient stability during pulmonary administration.

3.5 Determination of expression of TfR

To confirm the expression of TfR on human ATC [53], human PBMCs were activated by anti-CD3 antibody (OKT3), and the expression of TfR was quantified by flow cytometry over time. On day 0 (Figure 5), the TfR expression was at a basal level in PBMCs whereas the TfR expression increased dramatically from day 1 to day 5 after activation. T

lymphocytes undergo rapid differentiation, proliferation, and up-regulate TfR (CD71) to meet their high consumption of iron [23]. The TfR expression level slowly decreased after day 5 post-activation, but a clearly increased level of TfR expression compared to day 0 was maintained up to day 14 post-activation. This observation may be due to the fact that T cells are activated very early and that activation also leads to proliferation [23, 54]. It is possible that a) the rate of proliferation and differentiation of T cells slows down after 5 days post-activation and that b) a percentage of activated T cells becomes apoptotic resulting in lower TfR levels compared to earlier time points. However, the activated status of T cells maintains a relatively high consumption of iron compared to the resting status [23].To characterize the lymphocyte population in PBMCs after activation and to confirm the high expression of TfR on T cells, on day 6 post-activation, activated PBMCs were immunologically counter-stained with antibodies against CD3 and CD71 (TfR). Of the total cell population, approximately 90% of the cells were CD3 positive, and within this population, more than 60% cells were TfR and CD3 dual positive cells confirming activation stimulates T cells to overexpress TfR (Figure S1). Overexpression of TfR was also observed in Jurkat cells (Figure 7A). These results suggest the possibility to target primary ATCs or Jurkat cells, as a surrogate T cell line, via TfR targeting strategy.

3.6 *In vitro* cellular uptake of polyplexes

To determine the targeting efficiency of Tf-PEI, primary ATCs were transfected for 24 h and the cellular uptake was quantified by flow cytometry. Tf-PEI polyplexes were formulated with Alexa Fluor 488 labeled siRNA (AF488-siRNA) at different N/P ratios (5, 7.5, 10, 15, 20). Unmodified PEI polyplexes and lipofectamine 2000 (LF) served as positive controls, and treatment with free siRNA and an untreated group were also included as negative controls. Initially, cellular uptake was determined at low N/P ratios (N/P= 5 & 7.5, Figure S2 A) at which 100% siRNA condensation was achieved by unmodified PEI but 80% and 100% condensation was achieved by Tf-PEI conjugates. Tf-PEI polyplexes can target ATCs, and significantly higher cellular uptake was observed compared with unmodified PEI at both N/P ratios, although only 80% siRNA were encapsulated inside Tf-PEI polyplexes at N/P 5 (Figure 2). These results were in line with our previously published results [25]. Moreover, ATC-selective delivery of Tf-PEI polyplexes was confirmed at higher N/P ratios (N/P 10, 15, 20) (Figure 6A). Increased cellular uptake of both PEI and Tf-PEI was observed with increasing N/P ratios from 10 to 20. Tf-PEI polyplexes achieved 3.2 fold, 4.5 fold and 4.1 fold higher cellular uptake compared to PEI polyplexes at N/P 10, 15, 20, respectively. Most importantly, Tf-PEI achieved 1.8 fold more efficient cellular uptake at N/P 20 than LF mediated siRNA delivery. PEI polyplexes can non-specifically associate on the cell surface due to electrical interaction between their positive surface charge and negative charge of cellular membranes and induce adsorptive endocytosis. This mechanism contributes to non-targeted cellular uptake. However, PEI polyplexes are not efficiently taken up by primary ATCs. These results agree with a previous report from our group which focused on the observation that Tf-PEI can selectively deliver siRNA to ATCs overexpressing TfR but not resting T cells which are TfR negative [25]. To estimate the percentage of extracellular fluorescence resulting from polyplexes that are bound but not internalized, 0.4% trypan blue quenching treatment was performed on ATCs treated by Tf-PEI (N/P 20), PEI (N/P 20), LF and free siRNA. As shown in Figure S2 B, the MFI slightly decreased in all trypan blue

treated groups except the LF group. This result suggests that only a limited amount of extracellular fluorescence is associated with the surface of the cells but most of the fluorescent polyplexes were taken up intracellularly. The slightly increased MFI of the LF treated group (Figure S2 B) could be explained by the fact that apoptotic cells with a damaged cell membrane are stained completely by trypan blue and therefore no longer are detected by flow cytometry. As it is known that LF has a strong cytotoxic effect, especially on primary cells, it is possible that the MFI was skewed to only viable cells which seem to have a slightly higher MFI. To validate our results in a cell culture model, transfection experiments were also performed in Jurkat cells, which are often used as a T cell model cell line. Jurkat cells are an immortalized lymphoma cell line, however, and not as hard-to-transfect as primary T cells. In agreement with the results obtained in ATCs, cellular uptake of Tf-PEI polyplexes in TfR-overexpressing Jurkat cells (Figure 7A) was also significantly higher than that of PEI polyplexes (Figure 7B). It needs to be noted, however, that the transfection efficiency of LF in Jurkat cells is higher than that of Tf-PEI polyplexes. The cellular endocytosis profile and molecular membrane composition of this immortalized cell line is expected to differ significantly from primary ATCs. Additionally, their viability under transfection is expected to be higher than that of ATCs which do not withstand the cytotoxic effects of commercially available transfection reagents. These characteristics may contribute to efficient transfection of Jurkat cell with LF, while primary ATCs are especially difficult to transfect cells [55] and benefit from active targeting.

3.7 *In vitro* transfection efficacy

Next, we investigated whether the significantly higher internalization of Tf-PEI polyplexes could induce a corresponding downregulation of a targeted gene. Therefore, ATCs or Jurkat cells were transfected by Tf-PEI and PEI polyplexes prepared with siRNA against GAPDH or scrambled siRNA at N/P 15, and LF was included as additional positive control. GAPDH gene expression was normalized by β-actin gene expression and quantified via real time PCR (RT-PCR). As shown in Figure 6B, GAPDH expression in ATCs treated with Tf-PEI/siGAPDH polyplexes was 2 fold less than after transfection with PEI/siGAPDH. Moreover, significant downregulation of GAPDH expression was observed in Tf-PEI/siGAPDH group compared with Tf-PEI/scrambled siRNA group and untreated control. In contrast, there was no significant difference of GAPDH expression among PEI/siGAPDH, PEI/scramble siRNA treated cells and the untreated group. Unmodified PEI polyplexes can undergo endocytosis mediated by electrostatic interaction between their positive surface charge and the negative charge of the cellular membrane as demonstrated in cellular uptake study. However, this limited internalization was not sufficient to induce significant sequence-specific gene silencing compared with receptor mediated endocytosis. LF was too toxic for primary ATCs, and it was impossible to isolate sufficiently intact RNA after transfection. Therefore, no viable results were obtained in ATCs and experiments were repeated in Jurkat cells. A similar outcome of GAPDH knock down was observed in Jurkat cells (Figure 7C). Due to the small size of primary T cells and resolution constraints, confocal laser scanning microscopy was performed in Jurkat cells. Images of cellular uptake of Tf-PEI, PEI, and LF polyplexes/lipoplexes revealed that receptor-mediated uptake of Tf-PEI/siRNA resulted in even distribution of siRNA within the cytoplasm of the cells (Figure S3 D), while delivery with PEI resulted in punctuated distribution (Figure S3 C). The point-shaped distribution of

siRNA in the transfected cells could be a sign of endosomal entrapment of the LMW-PEI complexes. If the polyplexes are indeed unable of endosomal release, this observation, taken together with the less efficient uptake of non-targeted polyplexes could be one reason for the lack of gene knockdown. According to the efficient uptake results, LF mediated the most efficient gene knock down in Jurkat cells, which, however, is not representative for the transfection of primary ATCs.

3.8 *In vivo* delivery of polyplexes

To further validate the possibility of pulmonary delivery of siRNA to ATCs via Tf-PEI, a murine model of allergen-induced asthma-like inflammatory reaction was established as shown in Figure 8A. Animals were i.t administrated on 4 consecutive days with Tf-PEI or PEI polyplexes prepared with Alexa Fluor 647 labeled siRNA (siRNA-AF647), and administration of free siRNA-AF647 was included as negative control on day 35-38 (Figure 8A). On day 39, lung function of animals was determined by PenH assay. Overall, the airway hyperresponsiveness (AHR) of asthmatic groups of animals was slightly higher than in corresponding saline-exposed, healthy groups of animals (Figure S4 A). Additionally, according to the AUC of airway responsiveness against methacholine concentration curve, mice within the asthmatic group treated with PEI/siRNA polyplexes showed the highest AHR which was significantly higher than within the corresponding healthy control. On the other hand, there is no significant difference between asthmatic mice treated with Tf-PEI/siRNA polyplexes and their corresponding healthy control group (Figure S4 B). This data may suggest that the treatment with positively charged PEI/siRNA polyplexes could have intensified the pre-existing lung inflammation in the asthmatic animals but not the treatment with Tf-PEI/siRNA polyplexes, which are shielded by the negatively charged glycoprotein. On day 40, BALF, BAL cells and lung cells were collected and processed for determining concentration of IL-5 and IL-13, or for immunostaining, respectively. BAL cell populations were differentiated following the immunostaining strategy shown in Figure S6 and Table S1. As shown in Figure 8 B, Tf-PEI polyplexes uptake in T cells was significantly higher than that in B cells and eosinophils. More importantly, cellular uptake of Tf-PEI polyplexes in T cells was 1.3 and 1.5 fold higher than that in macrophages and type II pneumocytes, one type of alveolar cells, respectively. It has to be taken into account that lung resident macrophages serve as first line of cellular defense in the deep lung [56] by actively phagocytosing foreign particles, which may result in a significant amount of polyplexes being cleared. Additionally, the large interaction surface of type II pneumocytes with aerosolized particles also increases their possibility to associate with polyplexes. Considering that activated macrophages have elevated levels of TfR [57] also and epithelial cells express TfR as well [58], Tf-PEI polyplexes demonstrated very efficient T cell-targeted delivery. In lung suspension cells, uptake of Tf-PEI polyplexes in T cells was 1.7 fold higher than PEI polyplexes in asthmatic animals (OVA group). Furthermore, cellular uptake of Tf-PEI polyplexes in T cells from asthmatic animals was significantly higher than in healthy animals (saline), which demonstrated minimal cellular uptake similar to free siRNA treatment group (Figure 8 C). Tf-PEI and 5k PEI polyplexes didn't show toxicity toward A549 cells, a lung epithelial cell line, at N/P ratios ranging from 1 to 40 as assessed by LDH release assay (Figure S4). However, as suggested above, intratracheal administration, especially of positively charged polyplexes could induce additional inflammation. To

Europe PMC Funders Author Manuscripts

evaluate the potential pro-inflammatory effects of polyplexes, IL-5 an IL-13 were determined by a mouse cytokine 20-plex panel. As shown in Figure 8 D, overall, IL-5 levels were higher in all asthmatic groups, which can be explained by the allergic inflammation induced by the OVA-sensitization and challenge. However, asthmatic animals treated with PEI polyplexes demonstrated significantly higher secretion of IL-5. On the other hand, no significant difference of secretion of IL-5 in Tf-PEI polyplexes and free siRNA treated OVA-sensitized animals was observed compared with healthy animals. Additionally, the levels of cytokines in OVA-sensitized animals treated with targeted polyplexes was not significantly different from untreated OVA-sensitized animals (data not shown). The same secretion profile were observed in IL-13 (Figure S7). These results agree with the airway hyperresponsiveness results (Figure S5 A, B) and suggest that the Tf-shielding of Tf-PEI polyplexes efficiently reduces the pro-inflammatory effect of PEI polyplexes in asthmatic animals. It is worth noting that the repeated treatment with low molecular weight PEI was tolerated very well in healthy animals (Figure 8D, S7). These results are in line with previous reports [27, 28].

4 Conclusion

This study is the first attempt to deliver siRNA selectively to activated T cells for asthma therapy. Tf-PEI polyplexes exhibited desired physicochemical properties and achieved selective delivery of siRNA to ATCs followed by successful induction of gene knockdown. Such selectivity was also confirmed in a murine asthma model. Our present work demonstrates the possibility to specifically deliver siRNA to ATCs via targeting TfR. Although repeated administration of a Tf conjugate of low molecular weight PEI was well tolerated in healthy animals and no toxicity was observed in our study, clinical application of PEI or its conjugates is still limited by concern of any possible toxicity. Therefore, after having established an efficient targeting strategy for primary T cells in the present paper, our next studies will be devoted to developing a more biocompatible polymer to replace PEI. Subsequently, therapeutic effects of downregulating clinically relevant genes such as the Th_2 transcription factor GATA-3 will be determined.

Supplementary Material

Refer to Web version on PubMed Central for supplementary material.

Acknowledgements

We are grateful to Dr. Anna Moszczynska and Bryan Killinger (Department of Pharmaceutical Sciences, Wayne State University) for generous use of lab equipment and technical support. This work was supported by the Wayne State Start-Up and ERC-2014-StG – 637830 to Olivia Merkel. Lawrence G. Lum was supported in part by grants from the National Cancer Institute (R01 CA 092334 and R01CA 140314). The NIH Center grant P30CA22453 supporting the Wayne State Microscopy, Imaging and Cytometry Resources (MICR) is gratefully acknowledged.

References

1. 2014. The Global Asthma Report, in, Global Asthma Network
2. Barnes PJ. Immunology of asthma and chronic obstructive pulmonary disease. Nat Rev Immunol. 2008; 8:183–192. [PubMed: 18274560]

3. Pelaia G, Vatrella A, Maselli R. The potential of biologics for the treatment of asthma. Nature reviews Drug discovery. 2012; 11:958–972. [PubMed: 23197041]
4. Barnes PJ. Pathophysiology of asthma. British journal of clinical pharmacology. 1996; 42:3–10. [PubMed: 8807137]
5. Ortega HG, Liu MC, Pavord ID, Brusselle GG, FitzGerald JM, Chetta A, Humbert M, Katz LE, Keene ON, Yancey SW. Mepolizumab treatment in patients with severe eosinophilic asthma. New England Journal of Medicine. 2014; 371:1198–1207. [PubMed: 25199059]
6. Krug N, Hohlfeld JM, Kirsten A-M, Kornmann O, Beeh KM, Kappeler D, Korn S, Ignatenko S, Timmer W, Rogon C. Allergen-Induced Asthmatic Responses Modified by a GATA3-Specific DNAzyme. New England Journal of Medicine. 2015
7. Rettig GR, Behlke MA. Progress toward in vivo use of siRNAs-II. Molecular Therapy. 2012; 20:483–512. [PubMed: 22186795]
8. Elbashir SM, Harborth J, Lendeckel W, Yalcin A, Weber K, Tuschl T. Duplexes of 21-nucleotide RNAs mediate RNA interference in cultured mammalian cells. nature. 2001; 411:494–498. [PubMed: 11373684]
9. Huang H, Lee C, Chiang B. Small interfering RNA against interleukin-5 decreases airway eosinophilia and hyper-responsiveness. Gene therapy. 2008; 15:660–667. [PubMed: 18305576]
10. Lee C-C, Huang H-Y, Chiang B-L. Lentiviral-mediated GATA-3 RNAi decreases allergic airway inflammation and hyperresponsiveness. Molecular therapy. 2008; 16:60–65. [PubMed: 17878900]
11. Kanasty R, Dorkin JR, Vegas A, Anderson D. Delivery materials for siRNA therapeutics. Nature materials. 2013; 12:967–977. [PubMed: 24150415]
12. Schoenborn J, Sekimata M, Weaver W, Wilson C. Transfection of primary mouse T cells for stimulation-dependent cytokine enhancer assays. 2007
13. Fra AM, Williamson E, Simons K, Parton RG. Detergent-insoluble glycolipid microdomains in lymphocytes in the absence of caveolae. Journal of Biological Chemistry. 1994; 269:30745–30748. [PubMed: 7982998]
14. Lamaze C, Dujeancourt A, Baba T, Lo CG, Benmerah A, Dautry-Varsat A. Interleukin 2 receptors and detergent-resistant membrane domains define a clathrin-independent endocytic pathway. Molecular cell. 2001; 7:661–671. [PubMed: 11463390]
15. Costello E, Munoz M, Buetti E, Meylan P, Diggelmann H, Thali M. Gene transfer into stimulated and unstimulated T lymphocytes by HIV-1-derived lentiviral vectors. Gene therapy. 2000; 7:596–604. [PubMed: 10819575]
16. Zhao Y, Zheng Z, Cohen CJ, Gattinoni L, Palmer DC, Restifo NP, Rosenberg SA, Morgan RA. High-efficiency transfection of primary human and mouse T lymphocytes using RNA electroporation. Molecular Therapy. 2006; 13:151–159. [PubMed: 16140584]
17. Thomas CE, Ehrhardt A, Kay MA. Progress and problems with the use of viral vectors for gene therapy. Nature Reviews Genetics. 2003; 4:346–358.
18. The delivery problem. Nature Biotechnology. 2006
19. O'neill M, Kennedy C, Barton R, Tatake R. Receptor-mediated gene delivery to human peripheral blood mononuclear cells using anti-CD3 antibody coupled to polyethylenimine. Gene therapy. 2001; 8:362–368. [PubMed: 11313812]
20. Ding Q, Si X, Liu D, Peng J, Tang H, Sun W, Rui M, Chen Q, Wu L, Xu Y. Targeting and liposomal drug delivery to CD40L expressing T cells for treatment of autoimmune diseases. Journal of Controlled Release. 2015; 207:86–92. [PubMed: 25839125]
21. Lee J, Yun K-S, Choi CS, Shin S-H, Ban H-S, Rhim T, Lee SK, Lee KY. T cell-specific siRNA delivery using antibody-conjugated chitosan nanoparticles. Bioconjugate chemistry. 2012; 23:1174–1180. [PubMed: 22607555]
22. Kumar P, Ban H-S, Kim S-S, Wu H, Pearson T, Greiner DL, Laouar A, Yao J, Haridas V, Habiro K. T cell-specific siRNA delivery suppresses HIV-1 infection in humanized mice. Cell. 2008; 134:577–586. [PubMed: 18691745]
23. Pelosi E, Testa U, Louache F, Thomopoulos P, Salvo G, Samoggia P, Peschle C. Expression of transferrin receptors in phytohemagglutinin-stimulated human T-lymphocytes. Evidence for a three-step model. Journal of Biological Chemistry. 1986; 261:3036–3042. [PubMed: 3005277]

24. Daniels TR, Bernabeu E, Rodríguez JA, Patel S, Kozman M, Chiappetta DA, Holler E, Ljubimova JY, Helguera G, Penichet ML. The transferrin receptor and the targeted delivery of therapeutic agents against cancer. Biochimica et Biophysica Acta (BBA)-General Subjects. 2012; 1820:291–317. [PubMed: 21851850]
25. Kim N, Nadithe V, Elsayed M, Merkel O. Tracking and treating activated T cells. Journal of drug delivery science and technology. 2013; 23:17–21. [PubMed: 24660025]
26. Lungwitz U, Breunig M, Blunk T, Göpferich A. Polyethylenimine-based non-viral gene delivery systems. European Journal of Pharmaceutics and Biopharmaceutics. 2005; 60:247–266. [PubMed: 15939236]
27. Werth S, Urban-Klein B, Dai L, Höbel S, Grzelinski M, Bakowsky U, Czubayko F, Aigner A. A low molecular weight fraction of polyethylenimine (PEI) displays increased transfection efficiency of DNA and siRNA in fresh or lyophilized complexes. Journal of Controlled Release. 2006; 112:257–270. [PubMed: 16574264]
28. Peng Q, Zhong Z, Zhuo R. Disulfide cross-linked polyethylenimines (PEI) prepared via thiolation of low molecular weight PEI as highly efficient gene vectors. Bioconjugate chemistry. 2008; 19:499–506. [PubMed: 18205328]
29. Yang J, Chen H, Vlahov IR, Cheng J-X, Low PS. Evaluation of disulfide reduction during receptor-mediated endocytosis by using FRET imaging. Proceedings of the National Academy of Sciences. 2006; 103:13872–13877.
30. Kircheis R, Kichler A, Wallner G, Kursa M, Ogris M, Felzmann T, Buchberger M, Wagner E. Coupling of cell-binding ligands to polyethylenimine for targeted gene delivery. Gene therapy. 1997; 4:409–418. [PubMed: 9274717]
31. Snyder SL, Sobocinski PZ. An improved 2, 4, 6-trinitrobenzenesulfonic acid method for the determination of amines. Analytical biochemistry. 1975; 64:284–288. [PubMed: 1137089]
32. Merkel O, Beyerle A, Librizzi D, Pfestroff A, Behr T, Sproat B, Barth P, Kissel T. Nonviral siRNA Delivery to the Lung: Investigation of PEG-PEI Polyplexes and Their In Vivo Performance. Molecular Pharmaceutics. 2009; 6:1246–1260. [PubMed: 19606864]
33. Merkel OM, Librizzi D, Pfestroff A, Schurrat T, Béhé M, Kissel T. In vivo SPECT and real-time gamma camera imaging of biodistribution and pharmacokinetics of siRNA delivery using an optimized radiolabeling and purification procedure. Bioconjugate chemistry. 2008; 20:174–182. [PubMed: 19093855]
34. Sel S, Wegmann M, Dicke T, Sel S, Henke W, Yildirim AÖ, Renz H, Garn H. Effective prevention and therapy of experimental allergic asthma using a GATA-3–specific DNAzyme. Journal of Allergy and Clinical Immunology. 121:910–916.e915. [PubMed: 18325571]
35. Wegmann M, Fehrenbach H, Fehrenbach A, Held T, Schramm C, Garn H, Renz H. Involvement of distal airways in a chronic model of experimental asthma, Clinical and experimental allergy. journal of the British Society for Allergy and Clinical Immunology. 2005; 35:1263–1271.
36. Neuhaus-Steinmetz U, Glaab T, Daser A, Braun A, Lommatzsch M, Herz U, Kips J, Alarie Y, Renz H. Sequential development of airway hyperresponsiveness and acute airway obstruction in a mouse model of allergic inflammation. International archives of allergy and immunology. 2000; 121:57–67. [PubMed: 10686510]
37. Merkel OM, Marsh LM, Garn H, Kissel T. Flow cytometry-based cell type-specific assessment of target regulation by pulmonary siRNA delivery. Methods in molecular biology (Clifton, N.J.). 2013; 948:263–273.
38. Breunig M, Lungwitz U, Liebl R, Goepferich A. Breaking up the correlation between efficacy and toxicity for nonviral gene delivery. Proceedings of the National Academy of Sciences. 2007; 104:14454–14459.
39. Camp E, Wang C, Little E, Watson P, Pirollo K, Rait A, Cole D, Chang E, Watson D. Transferrin receptor targeting nanomedicine delivering wild-type p53 gene sensitizes pancreatic cancer to gemcitabine therapy. Cancer gene therapy. 2013; 20:222–228. [PubMed: 23470564]
40. Ogris M, Steinlein P, Kursa M, Mechtler K, Kircheis R, Wagner E. The size of DNA/transferrin-PEI complexes is an important factor for gene expression in cultured cells. Gene therapy. 1998; 5:1425–1433. [PubMed: 9930349]

41. Ogris M, Brunner S, Schüller S, Kircheis R, Wagner E. PEGylated DNA/transferrin-PEI complexes: reduced interaction with blood components, extended circulation in blood and potential for systemic gene delivery. Gene therapy. 1999; 6:595–605. [PubMed: 10476219]
42. Cardoso A, Simoes S, De Almeida L, Pelisek J, Culmsee C, Wagner E, Pedroso de Lima M. siRNA delivery by a transferrin-associated lipid-based vector: a non-viral strategy to mediate gene silencing. The journal of gene medicine. 2007; 9:170–183. [PubMed: 17351968]
43. Zhang X, Koh CG, Yu B, Liu S, Piao L, Marcucci G, Lee RJ, Lee LJ. Transferrin receptor targeted lipopolyplexes for delivery of antisense oligonucleotide g3139 in a murine k562 xenograft model. Pharmaceutical research. 2009; 26:1516–1524. [PubMed: 19291371]
44. Elsayed M, Corrand V, Kolhatkar V, Xie Y, Kim NH, Kolhatkar R, Merkel OM. Influence of oligospermines architecture on their suitability for siRNA delivery. Biomacromolecules. 2014; 15:1299–1310. [PubMed: 24552396]
45. Cherng J-Y, van de Wetering P, Talsma H, Crommelin DJ, Hennink WE. Effect of size and serum proteins on transfection efficiency of poly ((2-dimethylamino) ethyl methacrylate)-plasmid nanoparticles. Pharmaceutical research. 1996; 13:1038–1042. [PubMed: 8842041]
46. Grayson ACR, Doody AM, Putnam D. Biophysical and structural characterization of polyethylenimine-mediated siRNA delivery in vitro. Pharmaceutical research. 2006; 23:1868–1876. [PubMed: 16845585]
47. Kircheis R, Wightman L, Schreiber A, Robitza B, Rössler V, Kursa M, Wagner E. Polyethylenimine/DNA complexes shielded by transferrin target gene expression to tumors after systemic application. Gene therapy. 2001; 8:28–40. [PubMed: 11402299]
48. Merkel OM, Zheng M, Debus H, Kissel T. Pulmonary gene delivery using polymeric nonviral vectors. Bioconjugate chemistry. 2011; 23:3–20. [PubMed: 21999216]
49. Harush-Frenkel O, Bivas-Benita M, Nassar T, Springer C, Sherman Y, Avital A, Altschuler Y, Borlak J, Benita S. A safety and tolerability study of differently-charged nanoparticles for local pulmonary drug delivery. Toxicology and applied pharmacology. 2010; 246:83–90. [PubMed: 20417650]
50. Merkel OM, Rubinstein I, Kissel T. siRNA Delivery to the lung: What's new? Advanced drug delivery reviews. 2014; 75:112–128. [PubMed: 24907426]
51. Goerke J. Pulmonary surfactant: functions and molecular composition. Biochimica et Biophysica Acta (BBA)-Molecular Basis of Disease. 1998; 1408:79–89. [PubMed: 9813251]
52. Son Y-J, McConville JT. Development of a standardized dissolution test method for inhaled pharmaceutical formulations. International journal of pharmaceutics. 2009; 382:15–22. [PubMed: 19665533]
53. Neckers LM, Cossman J. Transferrin receptor induction in mitogen-stimulated human T lymphocytes is required for DNA synthesis and cell division and is regulated by interleukin 2. Proc Natl Acad Sci U S A. 1983; 80:3494–3498. [PubMed: 6304712]
54. Neckers, LM.; Cossman, J. Transferrin receptor induction in mitogen-stimulated human T lymphocytes is required for DNA synthesis and cell division and is regulated by interleukin-2 (TCGF). Thymic Hormones and Lymphokines. Springer; 1984. p. 383-394.
55. Christopher W, Jamie S, Masayuki S, William W. Transfection of primary mouse T cells for stimulation-dependent cytokine enhancer assays. Protocol Exchange. 2007; doi: 10.1038/nprot.2007.236
56. Kopf M, Schneider C, Nobs SP. The development and function of lung-resident macrophages and dendritic cells. Nature immunology. 2015; 16:36–44. [PubMed: 25521683]
57. Testa U, Petrini M, Quaranta M, Pelosi-Testa E, Mastroberardino G, Camagna A, Boccoli G, Sargiacomo M, Isacchi G, Cozzi A. Iron up-modulates the expression of transferrin receptors during monocyte-macrophage maturation. Journal of Biological Chemistry. 1989; 264:13181–13187. [PubMed: 2473988]
58. Curiel DT, Agarwal S, Romer M, Wagner E, Cotten M, Birnstiel ML, Boucher RC. Gene transfer to respiratory epithelial cells via the receptor-mediated endocytosis pathway. Am J Respir Cell Mol Biol. 1992; 6:247–252. [PubMed: 1540389]

Europe PMC Funders Author Manuscripts

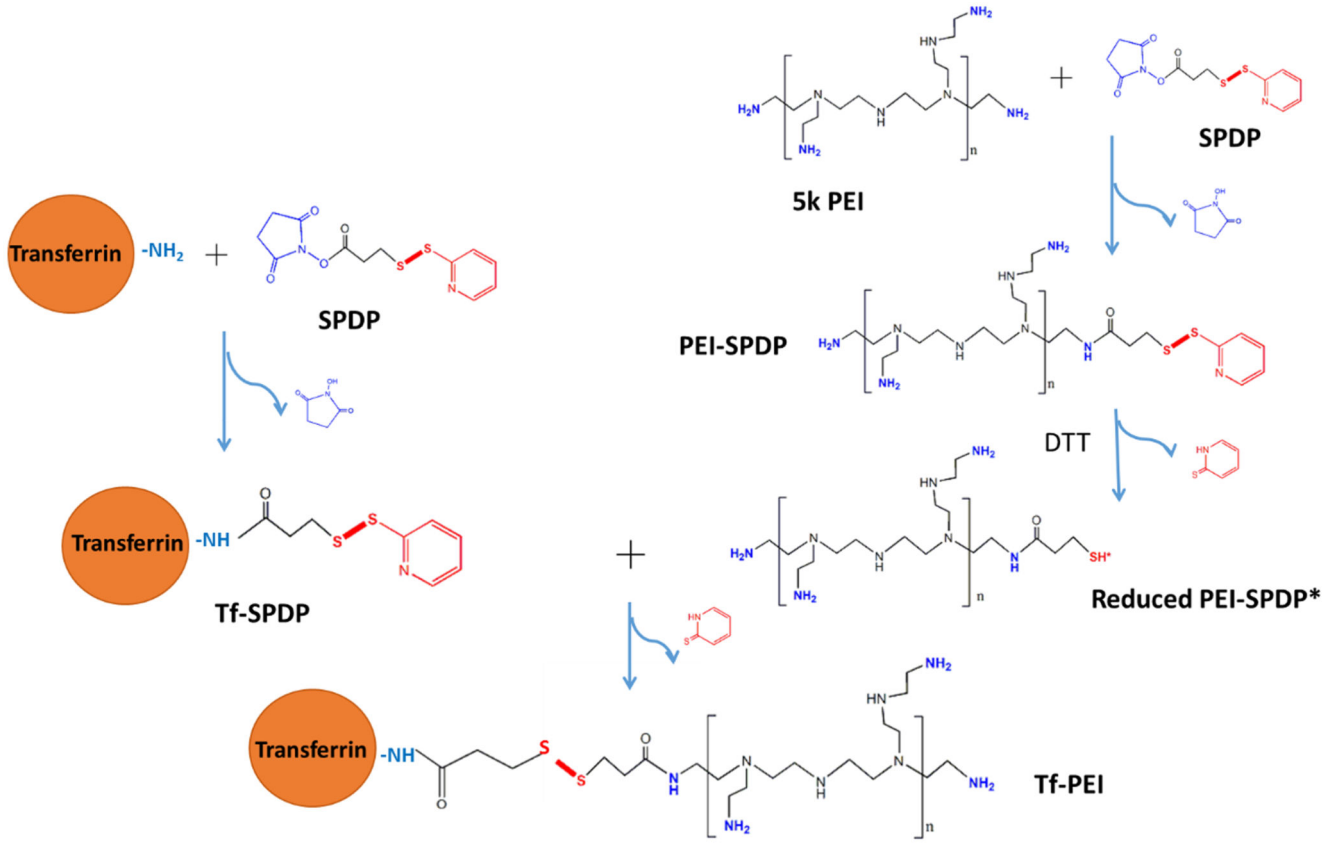

Fig. 1.

Synthesis scheme of transferrin-coupled polyethylenimine (Tf-PEI). Transferrin (Tf, left side) and PEI (right side) are reacted with N-succinimidyl 3-(2-pyridyldithio)-propionate (SPDP) in separate reactions. PEI-SPDP is activated by dithiothreitol (DTT) and coupled with Tf-SPDP to form a disulfide bond and the resulting Tf-PEI.

Europe PMC Funders Author Manuscripts

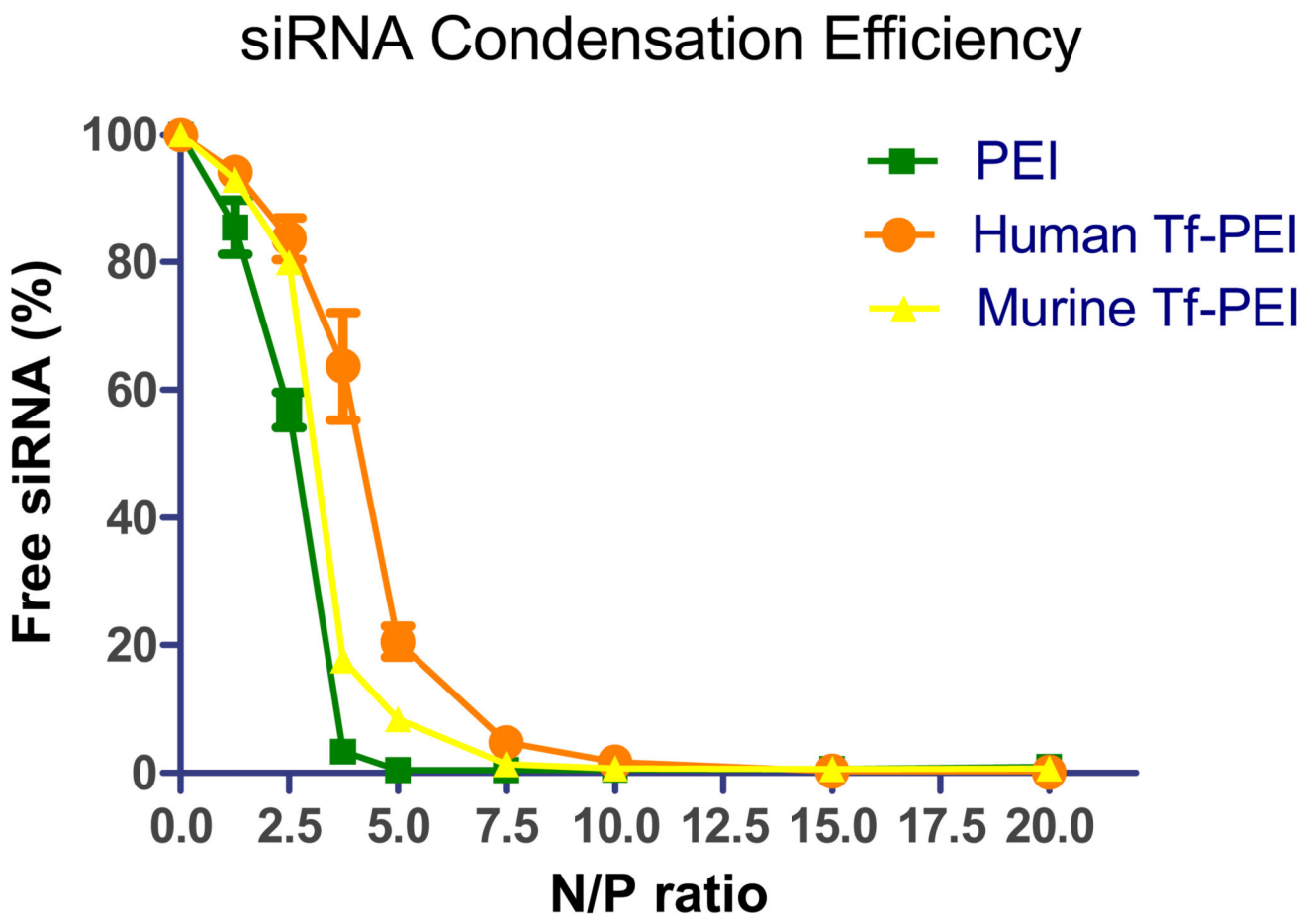

Fig. 2.

The siRNA condensation efficiency of PEI and Tf-PEI was measured by SYBR gold assay at different N/P ratios: 0, 1.25, 2.5, 3.75, 5, 7.5, 10, 15, 20. Fluorescence of free siRNA (N/P= 0) represents 100% free siRNA. (Data points indicate mean +/− SD, n= 2-3; Green square: PEI polyplexes, orange circle: human Tf-PEI, yellow triangle: murine Tf-PEI)

Europe PMC Funders Author Manuscripts

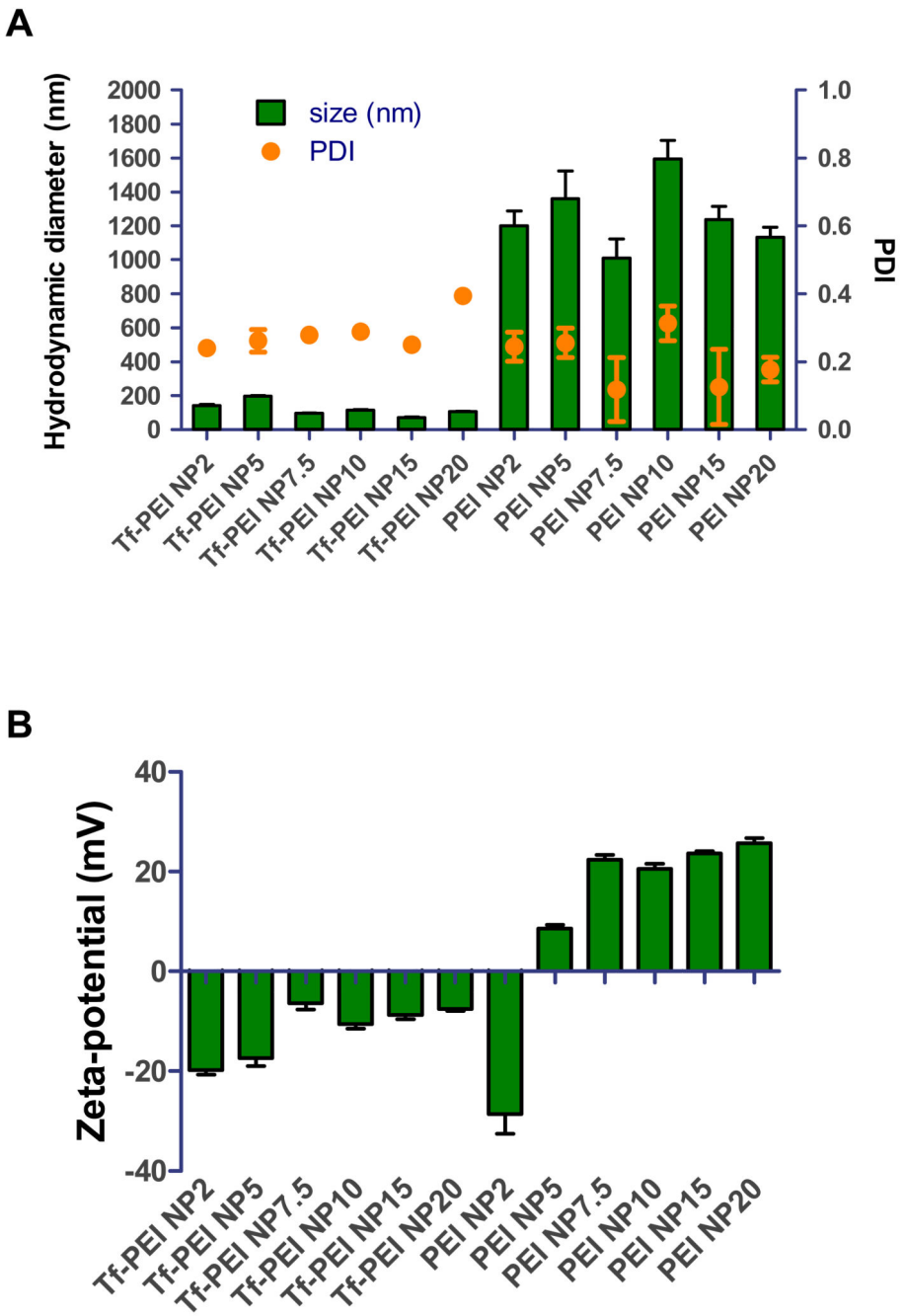

Fig. 3.

(A) Hydrodynamic diameters (left x-axis) and polydispersity indices (PDI, right x-axis) and (B) zeta-potentials of Tf-PEI and PEI polyplexes formulated with 50 pmol siRNA in HEPES buffered saline at different N/P ratios :2, 5, 7.5, 10, 15, 20. (Data points indicate mean +/− SD, n=3)

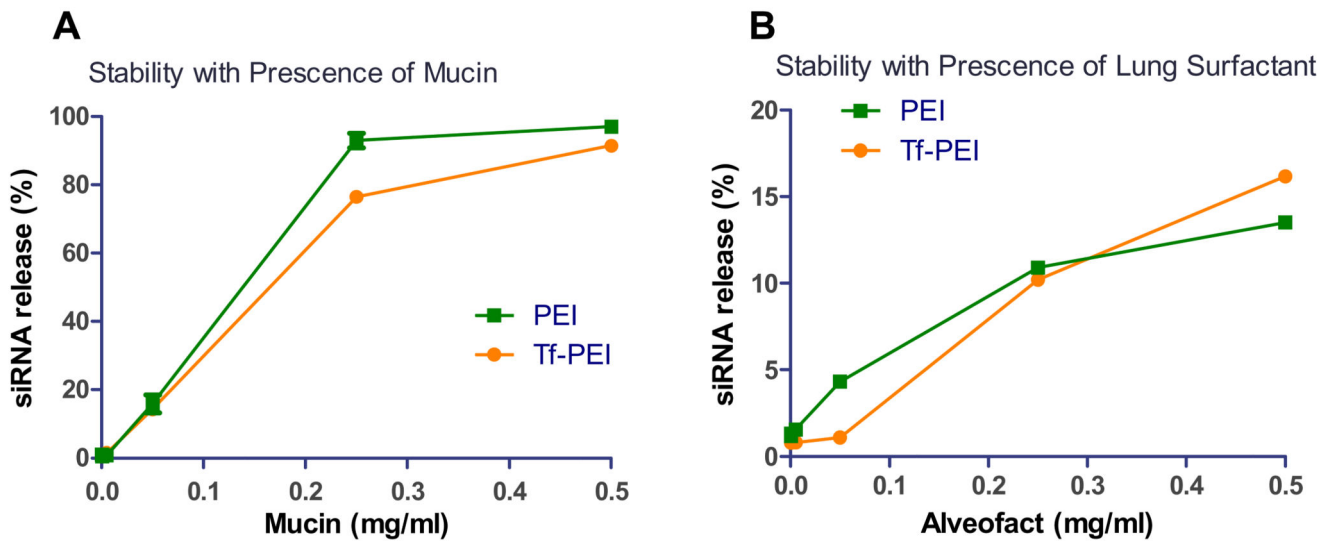

Fig. 4.

Stability of Tf-PEI and PEI polyplexes at N/P 7.5 was determined by modified SYBR gold assay after 20 min incubation with increasing concentration of (A) mucin and (B) lung surfactant (0.005-0.5 mg/ml). Free siRNA represents 100% siRNA release. (Data points indicate mean +/− SD, n=3; Green square: siRNA release from PEI polyplexes, orange circle: siRNA release from Tf-PEI polyplexes)

Europe PMC Funders Author Manuscripts

Europe PMC Funders Author Manuscripts

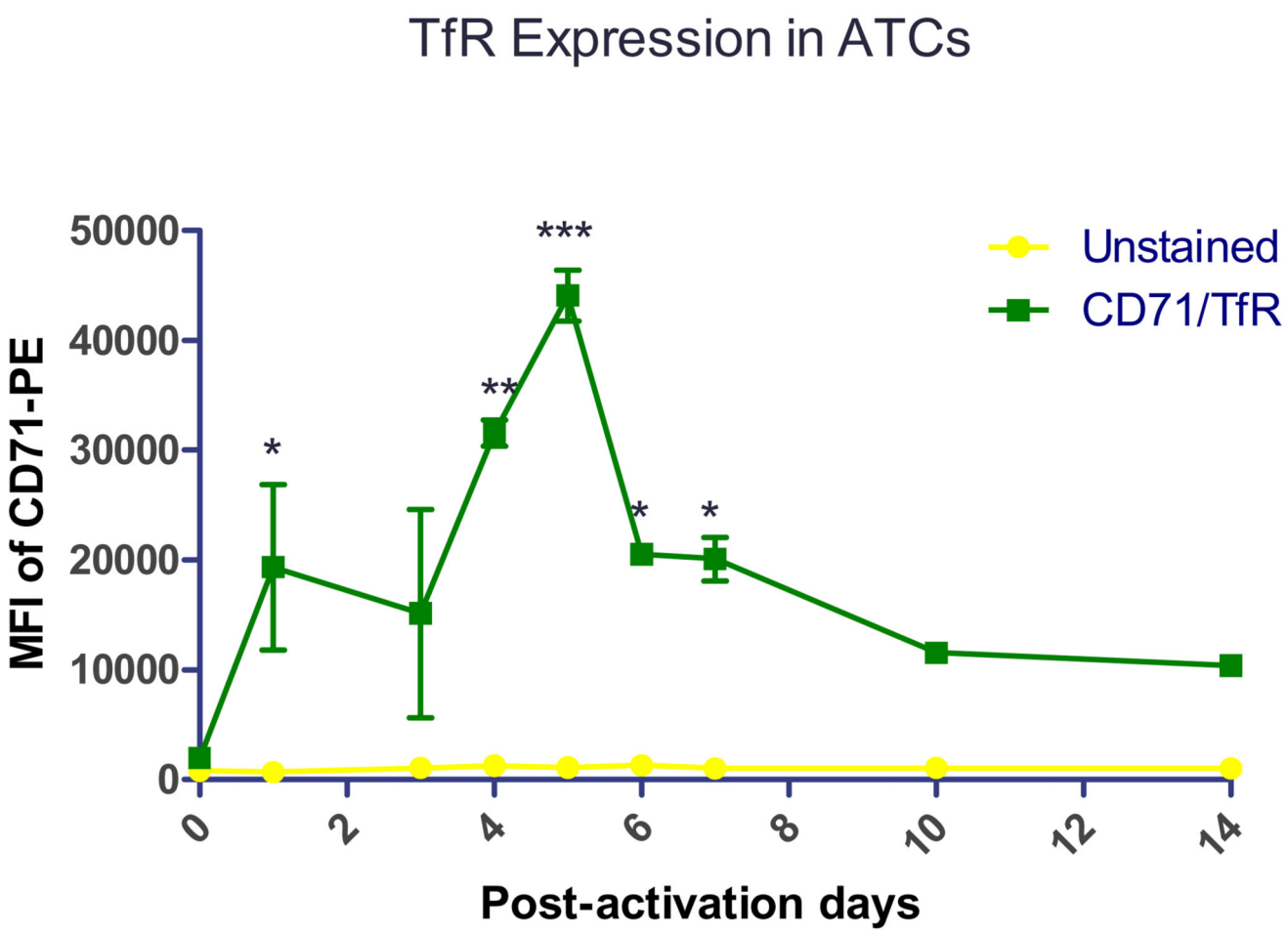

Fig. 5.

Human peripheral blood mononuclear cells (PBMCs) were activated by anti-CD3 antibody (OKT3) and were stained with anti-CD71 antibody to determine the expression of CD71, namely transferrin receptor (TfR), on different post activation days. The median fluorescence intensity (MFI) of CD71 of cells were quantified by flow cytometry. (Data points indicate mean +/− SD, n=1-3; Compared with D0, *, $p< 0.05$, **, $p < 0.01$, ***, $p<0.005$; Green square: MFI of PBMCs stained with CD71 antibody, yellow circle: background MFI of PBMCs not stained with antibody).

Europe PMC Funders Author Manuscripts

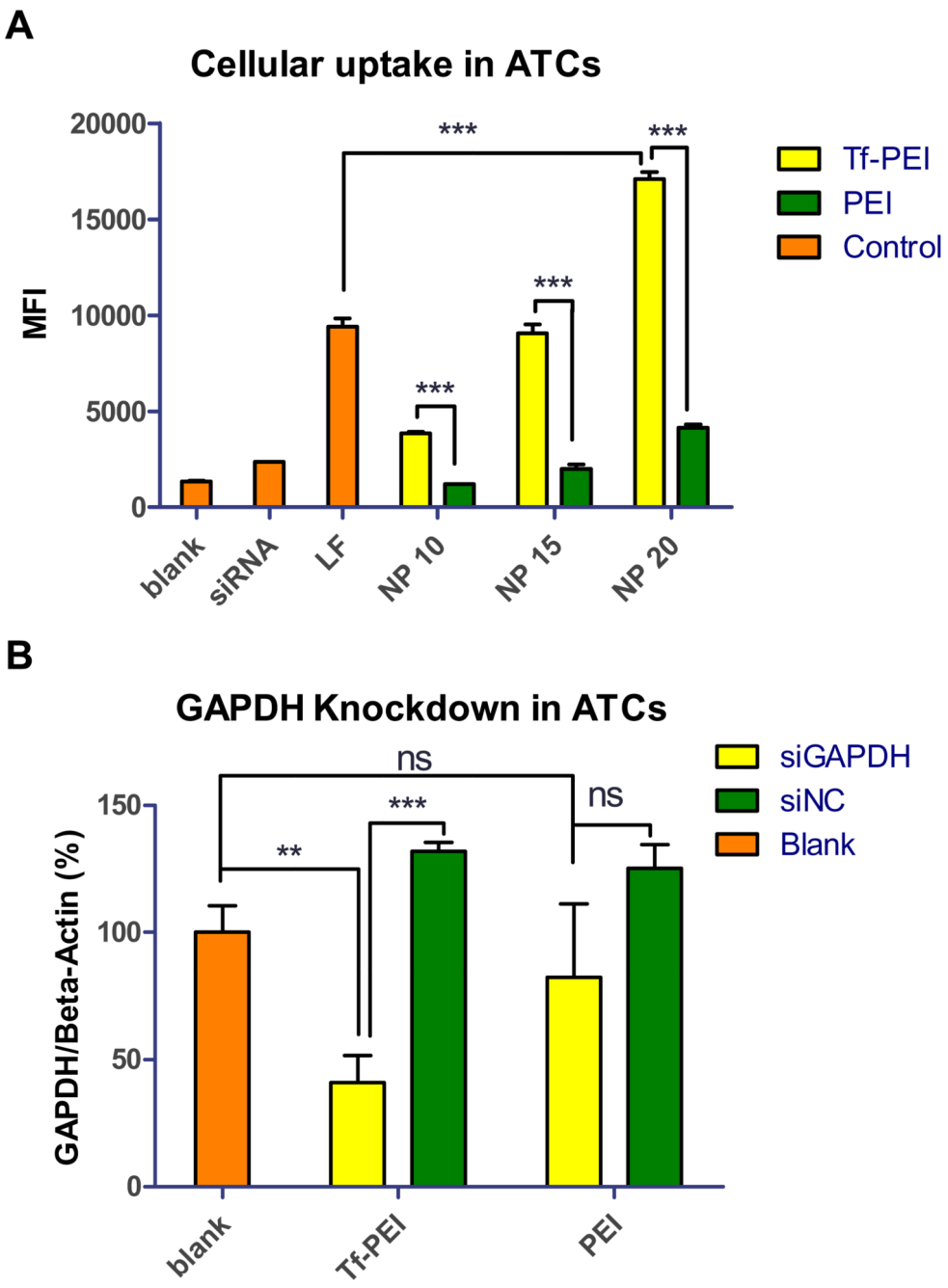

Fig. 6.

(A) Median fluorescence intensity (MFI) was determined by flow cytometry to evaluate the cellular uptake in primary human activated T cells (ATCs) of Tf-PEI, PEI and lipofectamine 2000 (LF) polyplexes/lipoplexes prepared with 50 pmol Alexa Fluor 488 labeled siRNA (AF488 siRNA) at different N/P ratios (10, 15, 20). (Data points indicate mean +/− SD, n >2; One-way ANOVA, **, $p < 0.01$, ***, $p<0.005$; Orange bar: control group including "blank" represents untreated cells, the "siRNA" group represents cells only treated with free siRNA, the "LF" group represents cells treated with LF lipolexes, yellow bars: cells treated

with Tf-PEI polyplexes, green bars: cells treated with PEI polyplexes). (B) GAPDH gene knockdown efficiency of Tf-PEI and PEI polyplexes at N/P 15 was validated in ATCs. GAPDH expression was normalized with beta-actin expression and quantified by real time PCR. (Data points indicate mean +/− SD, n =3; One-way ANOVA, **, $p < 0.01$, ***, $p<0.005$; Orange bars: the blank group represents GAPDH expression of untreated cells, yellow bars: GAPDH expression of the group treated with polyplexes containing siRNA against GAPDH (siGAPDH), green bars: negative control group, GAPDH expression of the group treated with polyplexes containing scrambled siRNA (siNC)).

Europe PMC Funders Author Manuscripts

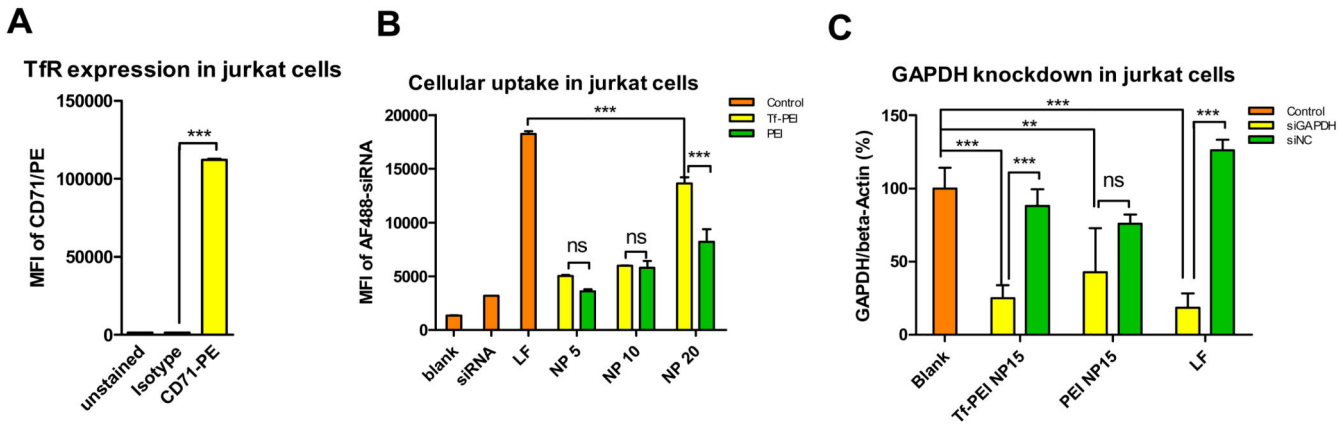

Fig. 7.

(A) Jurkat cells were stained with anti-CD71 antibody (TfR) or isotype antibody. The median fluorescence intensity (MFI) of antibody-stained of cells was quantified by flow cytometry. (Data points indicate mean +/− SD, n=2; One-way ANOVA, ***, p<0.005; Yellow bar: MFI of Jurkat cells stained with CD71 antibody, green bar: MFI of Jurkat cells stained with isotype antibody, orange bar: background MFI of Jurkat not stained with antibody). (B) Cellular uptake in Jurkat cells of Tf-PEI, PEI and lipofectamine 2000 (LF) polyplexes/lipoplexes prepared with 50 pmol AF488 siRNA at different N/P ratios (5, 10, 20) was quantified by flow cytometry (Data points indicate mean +/− SD, n=2; One-way ANOVA, ***, p<0.005; Orange bars: control groups include a “blank” group of untreated cells, the “siRNA” group are cells only treated with free siRNA, the “LF” group represents cells treated LF lipolexes, yellow bars: cells treated with Tf-PEI polyplexes, green bars: cells treated with PEI polyplexes). (C) GAPDH gene knockdown efficiency of Tf-PEI (N/P 15) was compared with PEI polyplexes (N/P 15) and LF lipoplexes. GAPDH expression was normalized with beta-actin expression and quantified by real time-PCR. (Data points indicate mean +/− SD, n =3; One-way ANOVA, **, p < 0.01, ***, p<0.005; Orange bar: the blank group represents GAPDH expression of untreated cells, yellow bars: GAPDH expression of cells treated with polyplexes/ lipoplexes containing siRNA against GAPDH (siGAPDH), green bars: negative control group, GAPDH expression of cells treated with polyplexes/ lipoplexes containing scrambled siRNA (siNC)).

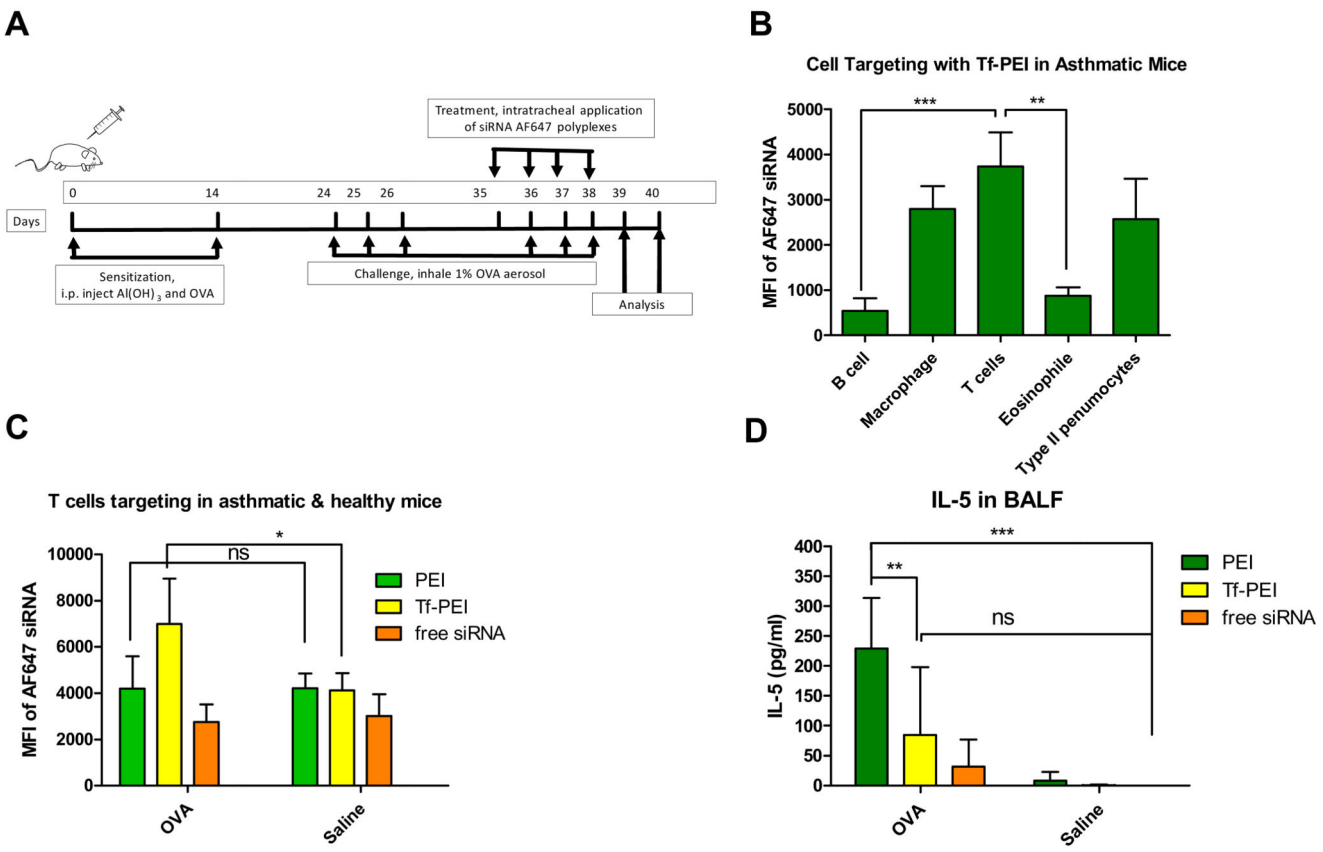

Fig. 8.

(A) Establishment of a murine asthma model. Balb/C mice were sensitized by i.p injection of $Al(OH)_3$ and ovalbumin (OVA) twice and challenged twice by inhalation of 1% OVA aerosol for 1 h daily for 3 consecutive days to induce airway inflammation. Animals treated by inhalation of saline served as healthy control. Polyplexes with 750 pmol Alexa Fluor 647 labeled siRNA (AF647 siRNA) were prepared with Tf-PEI or PEI at N/P 7.5 and applied intratracheally (i.t.), and free AF647 siRNA served as negative control. Lung function was determined on day 39. Bronchoalveolar lavage fluid (BALF), BALF cells and lung cells suspension were analyzed on day 40. (B) Cellular uptake of Tf-PEI polyplexes in different BALF cell populations from OVA sensitized-animals and (C) Cellular uptake of Tf-PEI polyplexes, PEI polyplexes and free AF647 siRNA in the T cell population of the lung cell suspensions from asthmatic and healthy mice was quantified by flow cytometry. (D) IL-5 levels in BALF were determined by the mouse cytokine 20-plex panel. (n>3, *, $p < 0.05$, **, $p < 0.01$, ***, $p<0.005$)

Europe PMC Funders Author Manuscripts